Polymer 50 (2009) 4241–4249

Contents lists available at ScienceDirect

Polymer

journal homepage: www.elsevier.com/locate/polymer

Sorption of lower alcohols in poly(ethylene terephthalate)

Preeti Chandra, William J. Koros*

School of Chemical and Biomolecular Engineering, Georgia Institute of Technology, Atlanta, GA 30332, USA

ARTICLE INFO

Article history:
Received 12 April 2009
Received in revised form
22 June 2009
Accepted 28 June 2009
Available online 3 July 2009

Keywords:
Sorption
Poly(ethylene terephthalate)
Prediction of transport properties

ABSTRACT

This paper presents equilibrium sorption and kinetics of lower alcohols in a 1.5 μ thick, biaxially oriented PET film. Methanol, ethanol, *n*-propanol and iso-propanol have been studied for the solubility and sorption kinetics in this film to understand how these properties change with penetrant size and branching. It is observed that *n*-propanol shows dual mode characteristics at all activities whereas the other three penetrants show Flory–Huggins uptake at high activities. Infinite dilution solubility is estimated and compared with that of esters, ketones and other hydrocarbons previously reported. The dispersive solubility parameter, δ_d is found to correlate well with the solubility of penetrants with the same functional group. The hydrogen bonding parameter, δ_h is observed to influence the solubility of penetrants with the same carbon number but different functional groups. This correlation with the solubility parameters may be extended to other functional groups and used to predict the infinite dilution solubility of larger penetrants in PET. Diffusion coefficients in the Fickian kinetics regime and Berens–Hopfenberg parameters in the non-Fickian kinetics regime have been evaluated. Diffusivity increases with concentration and decreases with size. Diffusion coefficient of iso-propanol is an order of magnitude lower than that of *n*-propanol due to branching effects.

Published by Elsevier Ltd.

1. Introduction

Poly(ethylene terephthalate) (PET) is a well known barrier material used for packaging of food, dairy products and beverages such as carbonated drinks, beer, juices. Growth in the packaged foods and beverages market has led to growth in the market for PET as well. In these products, retention of taste imparted by the flavor molecules is of great importance. The flavor is lost either due to flavor scalping or chemical degradation. To estimate the extent flavor scalping, knowledge of the transport properties of the species is essential. However, measurement of the transport properties of flavor molecules, which are large organic compounds, is difficult due to the low diffusivities, which translate into very long experiment times [1]. As a result, actual flavor molecules are much less studied and development of predictive capabilities gains significance. A potential route to prediction is the correlation of transport properties of small organic species in PET with their physical properties and subsequent extrapolation to larger molecules. Researchers have reported the solubility and diffusivity of a series of organic molecules such as linear and branched alkanes (*n*-butane, *i*-butane, *n*-pentane and *i*-pentane), linear and branched ketones (acetone, methyl ethyl ketone, methyl isopropyl ketone and methyl *n*-propyl ketone), linear esters (ethyl acetate and methyl acetate), acetaldehyde, benzene and toluene at different penetrant activities in biaxially oriented, semicrystalline PET. Solubility and diffusivity of liquid methanol, acetone, dimethyl formamide, dioxane and methylene chloride have also been studied [1–7]. Correlation of solubility and diffusivity of these penetrants with critical constants has been proposed by Dhoot and coworkers [1]. Upon examination of the correlation of solubility with critical temperature or Lennard–Jones force constant, it was observed that the properties of the polar molecules deviate significantly from the fit which may lead to large inaccuracies in the solubility estimation. It is, therefore desirable to develop another correlation which will allow better estimation of the properties of polar, condensable molecules [1,8].

This paper presents systematic study of equilibrium sorption and kinetics of lower alcohols in the 1.5 μ thick, biaxially oriented PET film. Methanol, ethanol, *n*-propanol and iso-propanol have been studied for the solubility and sorption kinetics in this film to understand how these properties change with increasing size of the penetrant and how branching may influence them. Sorption isotherms and kinetics have been discussed and correlation of the penetrant solubility with various thermodynamic constants has been investigated to understand the structure property relationships of small interacting penetrants. Quantities that have the best correlation and may be used for prediction purposes have been proposed.

---

* Corresponding author. Tel.: +1 404 385 2845; fax: +1 404 385 2683.
E-mail address: wkoros@chbe.gatech.edu (W.J. Koros).

0032-3861/$ – see front matter Published by Elsevier Ltd.
doi:10.1016/j.polymer.2009.06.066

2. Experimental

2.1. Materials characterization

A biaxially oriented, semicrystalline PET, 1.5 ± 0.15μ thick film, procured from GoodFellow Co., was used in this study. (Devon, PA). Methanol (99.9% ACS grade), ethanol (anhydrous, 99.5%), 1-propanol (≥99.80%) and 2-propanol (anhydrous 99.5%) were purchased from Sigma–Aldrich for the sorption experiments. Table 1 shows some relevant properties of the penetrants.

The density of the film, obtained using a density gradient column (Techne™, Burlington, NJ) filled with calcium nitrate-water solution was measured to be 1.3914 g/cc. The crystalline weight fraction was calculated from the sample density (ρ) using the two-phase model represented in equation (1). The amorphous phase density (ρ_a) is taken to be 1.331 g/cc and the density of PET crystals (ρ_c) is taken to be 1.455 g/cc [9], resulting in estimated crystalline fraction of 51%.

$$X_c = \left(\frac{\rho - \rho_a}{\rho_c - \rho_a}\right)\frac{\rho_c}{\rho} \tag{1}$$

Crystallinity was also calculated to be 51% using wide angle X-ray diffraction studies which were performed on a Rigaku Micro Max 002 system. Cu Kα X-ray source with Ni filter was used. Glass transition temperature was measured using differential scanning calorimetry performed DSC 220C from Seiko Instruments (Horsham, PA). First scans at a heating rate of 10 °C/min were taken. Glass transition occurred at 79 °C is close to the T_g of PET, usually reported between 70 and 85 °C. Melting temperature (T_m) of 257 °C also matches well with the typically reported T_m of 245–265 °C. Crystallinity was also estimated from DSC and was found to be lower at 31%. This may be attributed to the difference in the measurement observed using different techniques such as DSC, WAXD etc. Literature references and a discussion of this observation are provided in [10].

2.2. Gravimetric vapor sorption

Equilibrium uptake and kinetics were measured at 35 °C using the McBain quartz spring apparatus [11]. Details of the experimental setup and the measurement methodology are discussed previously [10]. The isotherms are obtained using the integral sorption method. Sorption kinetics is obtained by recording the spring position at different times after introduction of the vapor at time $t = 0$. Equilibrium is assumed to be attained when the spring position does not change over the course of 24 h. Once equilibrium is reached, the pressure is increased by introducing more vapors during sorption. The concentration of methanol in the polymer (C, ccSTP/ccpoly) is calculated using equation (2).

$$C = \left(\frac{K\Delta x}{g}\right)\frac{22414 \times \rho_p}{M_W \times M_p} \tag{2}$$

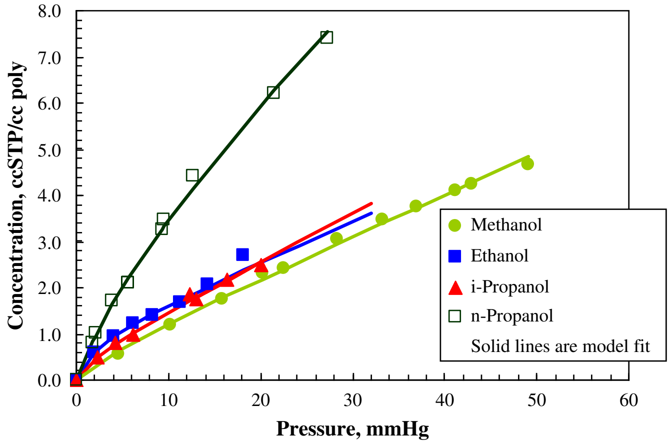

Fig. 1. Dual mode region of the sorption isotherm of MeOH, EtOH, *i*-PrOH and *n*-PrOH.

K (g/s^2) is the calibration constant of the spring, g (cm/s^2) is the rate of acceleration due to gravity, Δx (cm) is the change in spring position, ρ_p (g/cc) is the polymer density, M_p (g) is the mass of the polymer sample hung on the spring, M_W is the molecular weight of the penetrant.

3. Results and discussion

3.1. Equilibrium sorption at low activities – dual model regime

In the low activity region, ethanol (EtOH) and iso-propanol (*i*-PrOH) show dual mode behavior (i.e. the isotherm is concave to the x-axis) up to an activity of 0.18 and 0.35 respectively. The dual mode model is a phenomenological theory according to which sorption in glassy polymers occurs in two domains, a non-equilibrium Langmuir's domain or 'holes' where microvoids of excess free volume are frozen in and, an equilibrium domain or Henry's Law region. It is represented by equation (3) below. C'_H is the saturation capacity of these holes, b is the affinity constant, and p is the pressure of the penetrant outside the polymer, C is the penetrant concentration in the polymer and k_D is Henry's Law solubility constant.

$$C = \frac{C'_H bp}{(1 + bp)} + k_D p \tag{3}$$

It has been shown previously by the authors that methanol (MeOH) uptake in 15.2 μm non-annealed semicrystalline, biaxially oriented PET follows dual mode model at low activities. Positive deviation from the dual mode model occurs at $p/p_o = 0.25$ [12]. p is the partial pressure of the vapor and p_o is the saturation vapor pressure at 35 °C. The overall isotherm of methanol and the physical properties of the thin biaxially oriented film are very similar to those of the thicker, non-annealed film [12]. The isotherms of the lower alcohols and the corresponding dual mode model fit are shown in Fig. 1. *N*-propanol (*n*-PrOH) shows dual mode

Table 1
Properties of lower alcohols and PET solubility parameter.

Property →, Penetrant ↓	Saturation vapor pressure at 35 °C, mmHg [33]	Molar volume, cc/mol	Critical temperature, K	Solubility parameter, MPa$^{1/2}$			
				δ_d	δ_p	δ_h	δ
Methanol [13]	202.3	40.7	518	15.1	12.3	22.3	29.7
Ethanol [13]	103.3	58.5	521	15.8	8.8	19.4	26.6
n-Propanol [13]	36.0	75.2	513	16.0	6.8	17.4	24.6
i-Propanol [13]	80.0	68.4	541.7	15.8	6.1	16.4	23.5
PET [34]	–	–	–	19.4	3.5	8.6	21.5

Table 2
Dual mode model parameters for lower alcohols.

Penetrant →, Parameter ↓	C_H', ccSTP/ccpoly	b, atm^{-1}	k_d, ccSTP/ccpoly/atm
Methanol	0.71 ± 0.11	144.4 ± 15.2	63.1 ± 2.1
Ethanol	0.95 ± 0.31	308.5 ± 177.6	64.6 ± 11.6
n-Propanol	2.33 ± 0.12	104.46 ± 21.89	159.8 ± 53.0
i-Propanol	0.47 ± 0.25	415.3 ± 51.2	80.56 ± 8.71

characteristics all the way up to $p/p_o = 0.91$, which was the maximum activity tested, while the other penetrants show positive deviation from dual mode at medium to high activities. Table 2 shows the dual mode parameters thus obtained.

Solubility of a penetrant generally increases with increasing condensability. This trend is seen in the case of lower alcohols since the sorbed concentration and k_d are highest in propanol ($p_o = 36$ mmHg) and lowest in methanol. There is very little difference between the sorption isotherms of ethanol and *i*-propanol, probably partially due to saturation pressures that are closer together than the others (103.3 and 80.0 mmHg respectively). This has been discussed in more detail later in this section. It is also possible that owing to shape of *i*-propanol, the enthalpy of sorption is less which causes a lower overall uptake. The mass sorption of *i*-propanol is, of course, higher at equivalent molar sorption due to the higher molecular weight of propanol vs. methanol or ethanol.

Since the objective of this work is to provide further insight into the prediction of sorption properties of larger compounds, it is important to compare the solubility of the alcohols with that of other available penetrants. Solubility of a penetrant depends on many factors including its condensability. Critical temperature and boiling temperature are very good measures of the penetrant condensability and, hence, are often used to compare the solubility of different penetrants. Fig. 2 shows the correlation between penetrant critical temperature (T_c) and its infinite dilution solubility, similar to what was proposed by Dhoot and coworkers [4]. Based on the dual mode model described in equation 3, at low pressures, with $p \rightarrow 0$, the infinite dilution solubility (S_a) is defined as the sum of k_d and C_H'b. In cases such as water, CH_2Cl_2 and CH_3CHO, S_a is evaluated from the data at low activities by assuming Henry's Law. For the purposes of comparison with various literature values, all the solubility values have been normalized by the amorphous fraction of the PET sample. Dhoot and coworkers propose a power law fit between the infinite dilution solubility and critical temperature. As can be seen from the solid line (exponential fit) in Fig. 2, a broad correlation exists between solubility and T_c; however there are significant deviations, especially for molecules with polar functional groups. For example, though CH_2Cl_2 and CH_3COOCH_3 have similar T_c values of 510 K, their S_a values are quite different. On the other hand, the solubility of the permanent gases correlates very well with T_c. Thus, it seems that the predicted solubility may be quite accurate using the exponential dependence on critical temperature for permanent gases. For large, condensable, polar penetrants, the error of the prediction may be large. Michaels and coworkers showed that solubility of permanent gases also correlates very well with the Lennard–Jones force constant (ε/k) [8]. However, for larger, polar penetrants, even that correspondence shows significant deviations. Therefore it becomes important to understand the factors which may lead to better prediction of the solubility of polar molecules.

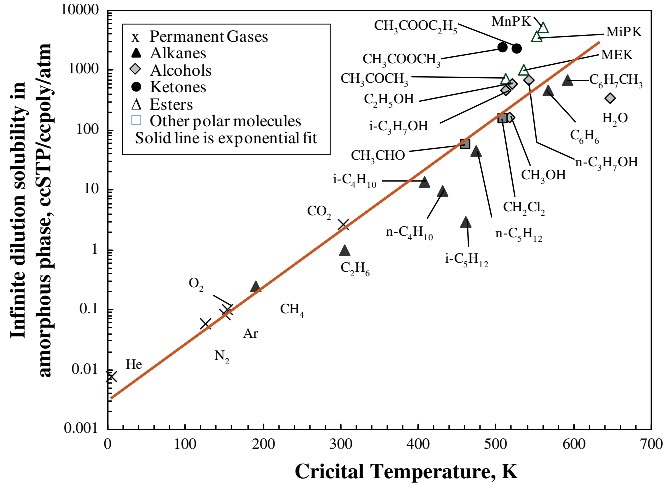

Fig. 2. Infinite dilution solubility of various penetrants in PET, normalized with respect to the amorphous fraction. (a) As a function of critical temperature, (b) As a function of Lennar–Jones force constant. Data for He, N_2, O_2, Ar, CH_4 and C_2H_6 have been taken from [8], CO_2 data from [9], acetone data from [24], CH_3COOCH_3, *i*-C_4H_{10}, $CH_3COOC_2H_5$, *i*-C_5H_{12} data from [1], MEK, MiPK, MnPK data from [3], *n*-C_4H_{10}, *n*-C_5H_{12} data from [4], C_6H_6 from [2], H_2O from [36], CH_2Cl_2 from [37] and CH_3CHO from [28]. All except water have been measured at 35 °C. Water was measured at 25 °C.

Hildebrand's solubility parameter is often used to establish mutual solubility of two solvents and to choose a good solvent for a particular polymer. This parameter depends on the cohesive energy density of the solvent molecule and can be decomposed into three substituent solubility parameters - dispersive (δ_d), permanent dipole–dipole interaction (δ_p) and hydrogen bonding parameters (δ_h) [13]. For the lower alcohols and PET, these values have been shown in Table 1. The overall solubility parameters δ is written as:

$$\delta^2 = \delta_d^2 + \delta_h^2 + \delta_p^2 \tag{4}$$

Despite the presence of the polar ester (–COO–) group in PET, the dipole-dipole interaction and hydrogen bonding parameters are not very large. The largest contribution comes from the dispersive solubility parameter, indicating that this, and not hydrogen bonding might be the dominant factor in PET. This is also evidenced by the water solubility in PET, which is much lower than the solubility in other polymers with polar groups such as ethylene vinyl alcohol, poly(methyl methacrylate), polyimides and poly(acrylonitrile) [14–20]. Fig. 3 shows the infinite dilution solubility of various classes of penetrants such as alcohols, ketones and hydrocarbons plotted against the penetrants' dispersive solubility parameter $(\delta_d - \delta_{d,PET})^2$. The δ_d values for the organic species have been taken from the Polymer Handbook [13], and the $\delta_{d,PET}$ is larger than all of these values. The solubility shows an excellent exponential correlation with the dispersive solubility parameter within

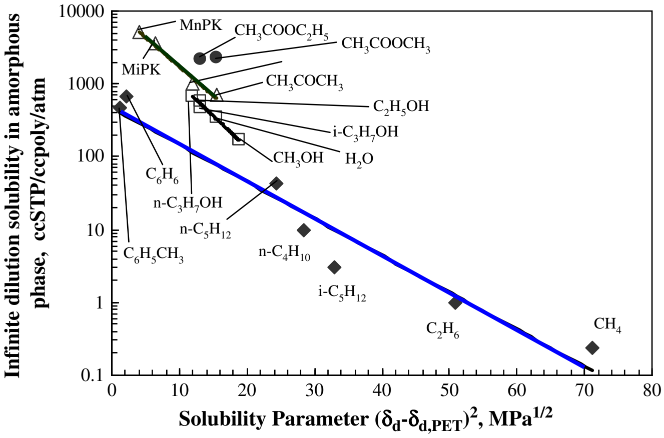

Fig. 3. Relationship of infinite dilution solubility in the amorphous phase with the dispersive solubility parameter. PET δ_d is 19.4 MPa$^{1/2}$. References are the same as in Fig. 1.

the same group of penetrants. Since only two data points are known for the esters, an exponential fit has not been made. It must be pointed out that even water solubility in PET lies on the same line as the alcohols. Water has very different overall properties with a very high value of $\delta_h = 42.7$ MPa$^{1/2}$ and cannot be considered with most organic molecules. However, the δ_d of water is similar to that of the alcohols. It is, therefore, encouraging to find that even water fits the correlation drawn with the dispersive solubility parameter. Fig. 3 shows that even for similar dispersive solubility parameter values, the trend of solubility is:

Esters > Ketones > Alcohols > Hydrocarbons

Since different functional groups lie along different lines, it may be hypothesized that the dipole–dipole interaction and hydrogen bonding ability play an important role in determining this trend in the solubility. With $\delta_{h,PET}$ being the second largest parameter, $(\delta_h - \delta_{h,PET})^2$ is considered. To investigate the correlation of this parameter across functional groups, Fig. 4 plots solubility vs. $(\delta_h - \delta_{h,PET})^2$ for C-3 and C-4 molecules. It is observed that for the same carbon length,

Solubility of Esters > Ketones > Alcohols > Hydrocarbons and $(\delta_h - \delta_{h,PET})^2$ of Esters < Ketones < Alcohols < Hydrocarbons.

This explains the relative solubility of alcohols and esters even though the δ_d is similar for the penetrants. As the carbon length increases, the correlation becomes stronger. Similar trends have also been reported for acetone and methyl acetate sorption in poly(*n*-butyl methacrylate) [21]. Hopfenberg and coworkers studied sorption of lower alcohols including *n*-PrOH and *i*-PrOH in PMMA at different temperatures and evaluated the enthalpy of sorption. They concluded that while hydrogen bonding may control the penetrant–penetrant interactions, it plays a smaller role in the penetrant–polymer interactions [22]. Similarly, for PET-lower alcohol systems, it seems that hydrogen bonding solubility parameter plays an important role in determining the solubility of the penetrants with the same carbon chain length. Such a correlation can become a useful tool for larger flavor molecules which usually have more than one functional group. However, to develop this correlation completely, two things are needed: (a) some other functionalities such as –COOH, –CHO, –O– and –C= need to be studied and plotted in a similar manner and, (b) flavor molecules are often cyclic compounds; therefore a few small cyclic molecules should also be added to this data base [23]. These investigations may lead to the identification of an additional dependence on δ_p, which is not evident in this case. Therefore, depending on the functional groups present and the number of carbon atoms, a penetrants' solubility may be predicted using Hansen solubility parameters. Of course, it must be emphasized that, all throughout, only infinite dilution solubility is being correlated. At higher activities, conditioning and swelling effects may lead to changes in the solubility based on the increased polymer chain mobility which makes it difficult to include in the correlation at present.

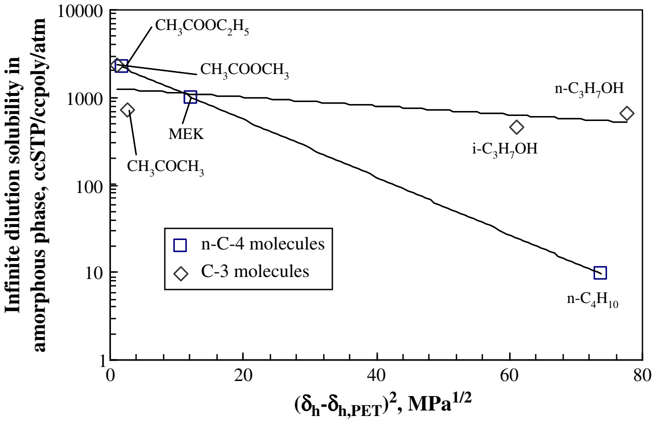

Fig. 4. Relationship of infinite dilution solubility of penetrants in amorphous phase with different functional groups with hydrogen bonding solubility parameter.

Attempts have also been made to correlate the affinity constant, *b*, in the dual mode model with various thermodynamic quantities such as critical temperature and the Lennard–Jones force constant (ε/k) [24]. For the permanent gases such as He, O_2, Ar, etc, the ε/k vs. log b has been shown to be linear for various polymers [25]. However, when all the polar molecules are also included, correlating with critical temperature seems to give a better fit as shown by the R^2 values of the exponential fit. This is shown in Fig. 5(a) and (b) for comparison. The critical temperature for the penetrants has been obtained from [26].

3.2. Equilibrium sorption at high activities

Sorption isotherms of methanol, ethanol and iso-propanol showed Flory–Huggins characteristics at higher activities. The complete sorption isotherms, plotted with respect to activity of the penetrant, are shown in Fig. 6. *N*-Propanol has been included in

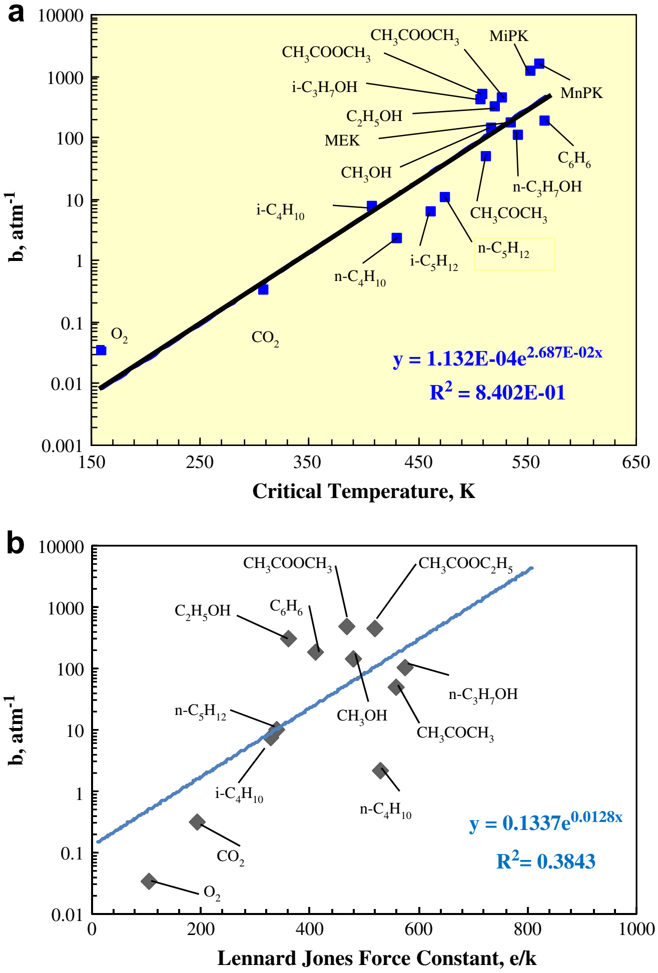

Fig. 5. (a) Correlation of affinity constant of various penetrants in PET with their critical temperature, (b) Correlation of affinity constant with Lennard–Jones force constant. The former is a better fit evidenced by the R^2 value.

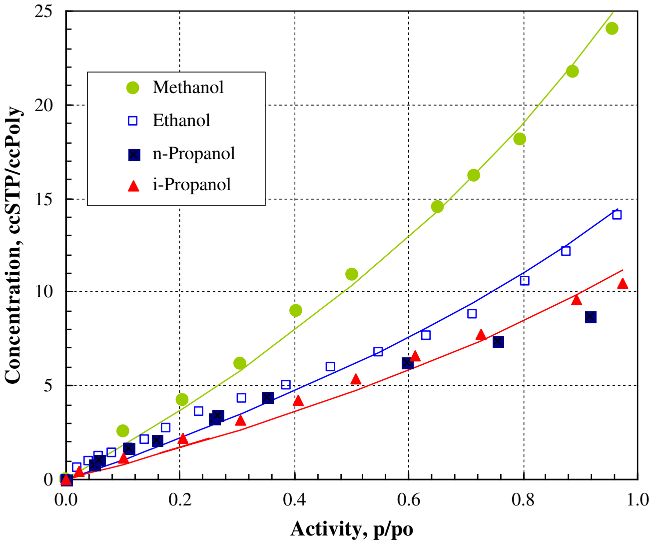

Fig. 6. Sorption isotherms of lower alcohols in PET. Solid lines are Flory–Huggins model fit with a constant interaction parameter χ.

the figure for comparison even though it shows dual mode characteristics up to $p/p_o = 0.90$. Flory–Huggins parameters are shown in Table 3. At similar activity levels, methanol has the highest sorption among the four penetrants and may be expected to swell the polymer more than the other molecules. Ethanol sorption is less than methanol but more than *n*- and *i*-propanol. It is interesting to note that the uptake of the propyl alcohols is very similar in the high activity range despite significantly different saturation pressures or volatility (80 mmHg for *i*-propanol vs. 36 mmHg for *n*-propanol). % Weight uptake at the highest activity of the penetrant is also shown in Table 3. These values are on a total polymer weight basis. Even though the sorbed concentration is higher for MeOH due to a smaller molecular weight, the weight % uptake is very similar for all the penetrants.

3.3. Sorption kinetics

As in the case of the methanol and amorphous PET system [12] where Fickian diffusion was observed at low activities and small concentration intervals, the thin, biaxially oriented film shows Fickian characteristics at low activities of methanol, ethanol and *n*- and *i*-propanol. However, significant relaxation effects are observed at higher activities. Fig. 7 shows the kinetics of EtOH, *i*-PrOH and *n*-PrOH at low partial pressures. Methanol sorption in the 1.5 μ thick film at low activities is not shown here because sorption equilibrium is reached rapidly when the kinetics are Fickian with diffusion coefficients of the order of 10^{-10} cm^2/s [12]. Based on the M_t/M_∞ vs. $t^{1/2}$ plots, diffusion coefficients have been evaluated for EtOH, *n*-PrOH and *i*-PrOH using Fick's Law for double sided sorption in flat films, as shown in equation (5). M_t is the mass uptake/removal at time t, M_∞ is the amount absorbed/desorbed at equilibrium, D is the diffusivity, t is the time elapsed since the start of sorption at $t = 0$ and l is the half thickness of the film. The values of D are shown in Table 4.

Table 3
Flory–Huggins interaction parameter and % weight uptake for lower alcohols.

Penetrant	Methanol	Ethanol	*n*-Propanol	Iso-propanol
Interaction parameter, χ	1.95 ± 0.01	2.10 ± 0.02	–	2.06 ± 0.03
Uptake at the highest activity measured, g/100 g poly	2.47	2.08	1.72	1.98

$$\frac{M_t}{M_\infty} = 1 - \frac{8}{\pi^2}\sum_{n=0}^{\infty}\frac{1}{(2n+1)^2}\exp\left[-\frac{(2n+1)^2\pi^2 Dt}{4l^2}\right] \tag{5}$$

As is to be expected with increasing penetrant size, the diffusion coefficients decrease in the following order in the low pressure range being considered.

$$\mathrm{MeOH}(10^{-10}\ \mathrm{cm^2/s}) > \mathrm{EtOH}(10^{-12}\ \mathrm{cm^2/s}) > n-\mathrm{PrOH}(10^{-13}\ \mathrm{cm^2/s}) > i-\mathrm{PrOH}(10^{-14}\ \mathrm{cm^2/s})$$

The difference in the position of the –OH group in *i*- and *n*-PrOH causes an order of magnitude decrease in the diffusion coefficient. The van der Waal's diameter and the dimensions of these molecules are shown below in Table 5. The van der Waal's diameter (units of nm) has been calculated using equation (6). The constant *v* (units of liter/mol) is the molar volume that is used in van der Waal's equation of state [27], and may be calculated using the critical temperature and pressure [26].

$$d_{\mathrm{vdW}} = 1.184v^{1/3} \tag{6}$$

Though the van der Waal's diameters of *i*-PrOH and *n*-PrOH have been calculated to be very similar, the changes in the dimensions of the two molecules clearly explain the reduction in the diffusivity of *i*-PrOH. The decreased diffusion coefficient is a result of the molecular shape of *i*-PrOH. Despite being shorter

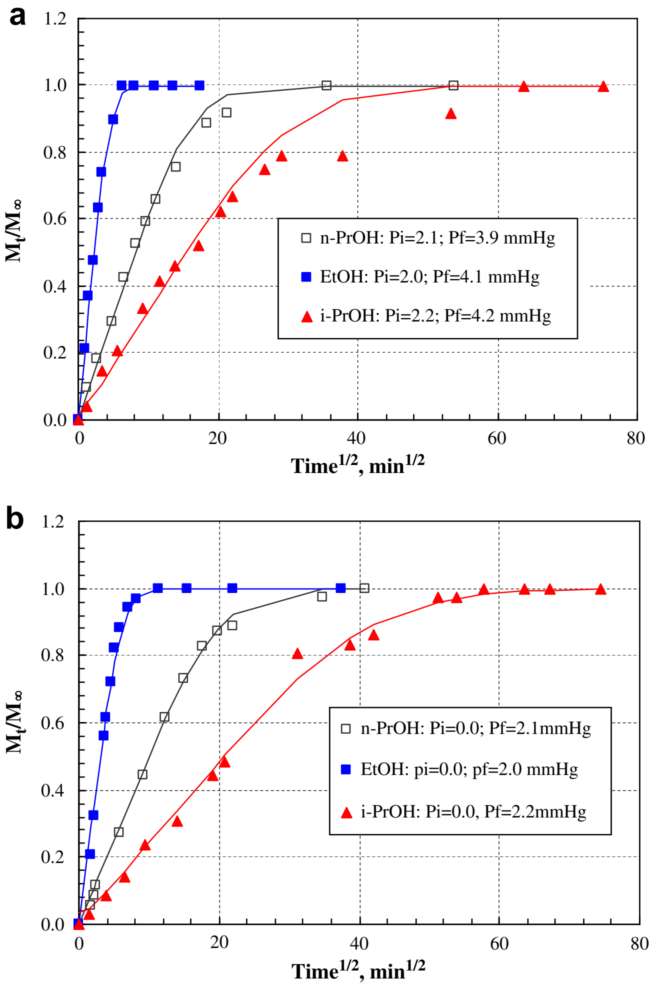

Fig. 7. Fickian diffusion of ethanol, *i*-propanol and *n*-propanol in the low pressure regime.

Table 4
Diffusion coefficient and Berens–Hopfenbeg parameters in methanol, ethanol, *i*-propanol and *n*-propanol.

Constant	MeOH	EtOH	*n*-PrOH	*i*-PrOH
Fickian kinetics in Fig. 7				
D, cm^2/s (2–4 mmHg)	Ref. [35]	$3.41 \pm 0.1 \times 10^{-12}$	$2.64 \pm 0.1 \times 10^{-13}$	$7.83 \pm 0.2 \times 10^{-14}$
D, cm^2/s (0–2 mmHg)	Ref. [35]	$1.91 \pm 0.1 \times 10^{-12}$	$1.79 \pm 0.1 \times 10^{-13}$	$1.91 \pm 0.1 \times 10^{-14}$
Two stage non-Fickian kinetics in Figs. 8–11				
Pressure range, P_i, P_f, mmHg	61.7, 82.5	40.2, 48.2	21.5,27.2	48.7,57.9
k_R, s^{-1}	8.77×10^{-6}	$1.43 \pm 0.1 \times 10^{-5}$	$3.35 \pm 0.13 \times 10^{-6}$	$2.73 \pm 0.13 \times 10^{-6}$
ϕ_f	0.40	0.53	0.32	0.36
D, cm^2/s	–	$6.16 \pm 0.5 \times 10^{-12}$	$9.42 \pm 1.4 \times 10^{-13}$	$6.32 \pm 0.9 \times 10^{-13}$
Pressure range, P_i, P_f, mmHg	145.0, 161.0	90.7, 99.8	27.2,33.0	71.3,77.6
k_R, s^{-1}	7.59×10^{-6}	$3.91 \pm 0.1 \times 10^{-6}$	$4.87 \pm 0.3 \times 10^{-6}$	$8.90 \pm 2.0 \times 10^{-6}$
ϕ_f	0.48	0.24	0.35	0.54
D, cm^2/s	–	$2.53 \pm 0.6 \times 10^{-11}$	$2.96 \pm 0.7 \times 10^{-12}$	$3.11 \pm 0.08 \times 10^{-12}$

than *n*-PrOH, iso-propanol is a much fatter molecule as is suggested by its greater width and height. This means that the molecule needs to expend more energy as its makes an activated jump. A higher energy penalty will result in decreased frequency of the jumps and, hence, a lower diffusion coefficient. Dhoot and coworkers observed that for hydrocarbons, *i*-butane has a lower diffusion coefficient than even *n*-pentane [1]. They conclude that branching influences the diffusivity more than an increase in the chain length by one carbon atom. It seems that the increase in the width and height of iso-butane molecule with respect to the *n*-butane structure is responsible for the lower diffusion coefficient than *n*-butane and *n*-pentane. These findings are consistent with our results for iso-propanol vs. *n*-propanol. Berens and Hopfenberg suggest that anisometric molecules, which have different orthogonal dimensions and are either flattened (e.g. benzene) or long (e.g. *n*-hexane), have greater mobility than the nearly spherical molecules. They conclude that the diffusivity of such molecules is governed by a dimension smaller than the mean penetrant diameter [27]. This could explain why, despite very similar van der Waal's diameter, *i*- and *n*-propanol have different diffusivities. They also propose the concept of a 'diffusion diameter', which is the diameter of a hypothetical spherical molecule that has the same diffusion coefficient. Though this approach takes into account the shape effect, as opposed to other correlations that may be drawn with the mean diameter estimated from liquid density and the critical or molar volume of the penetrant, it suffers from the disadvantage that the 'diffusivity diameter' is not known for all penetrants. Moreover, the diameter evaluated by Berens and Hopfenberg for the same species in different glassy polymers often has different values [27]. Therefore, it appears that the correlation with critical or mean diameter may be more useful despite the possibility of a large error in the predicted diffusivity of polar molecules [28,27].

At intermediate and high activities, relaxation effects have been observed in the kinetics of all the penetrants. Relaxation effects are usually observed due to the increase in polymer chain mobility induced by the sorbed penetrant. As the polymer chain mobility increases, further uptake of the penetrant is observed leading to two distinct stages in the uptake kinetics - Fickian diffusion controlled and relaxation controlled. Lower alcohols show such effects which have also been observed for sorption of other penetrants such as benzene, acetone and methyl acetate etc in PET [2,3]. Other polymer penetrant systems which show such a behavior include polystyrene-*n*-hexane, poly(vinyl alcohol)-vinyl chloride and many others [29,30]. Even sorption of D-limonene in oriented, rubbery poly-propylene shows such non-Fickian characteristics which suggest that sorption kinetics of large aroma flavors is influenced by the polymer chain relaxation [31]. Figs. 8–11 show representative kinetics for methanol, ethanol, *n*-propanol and *i*-propanol respectively. These two stage effects in the PET-lower alcohols system have been modeled using the Berens–Hopfenberg

Table 5
Dimensions of lower alcohols.

Penetrant	van der Waal's diameter, (Å)	Dimensions, $l \times w \times h$ (Å)
Methanol	4.78	4.6 × 3.8 × 3.5
Ethanol	5.25	6.0 × 3.8 × 4.0
n-Propanol	5.65	6.3 × 5.4 × 4.9
i-Propanol	5.69	7.5 × 3.8 × 4.2

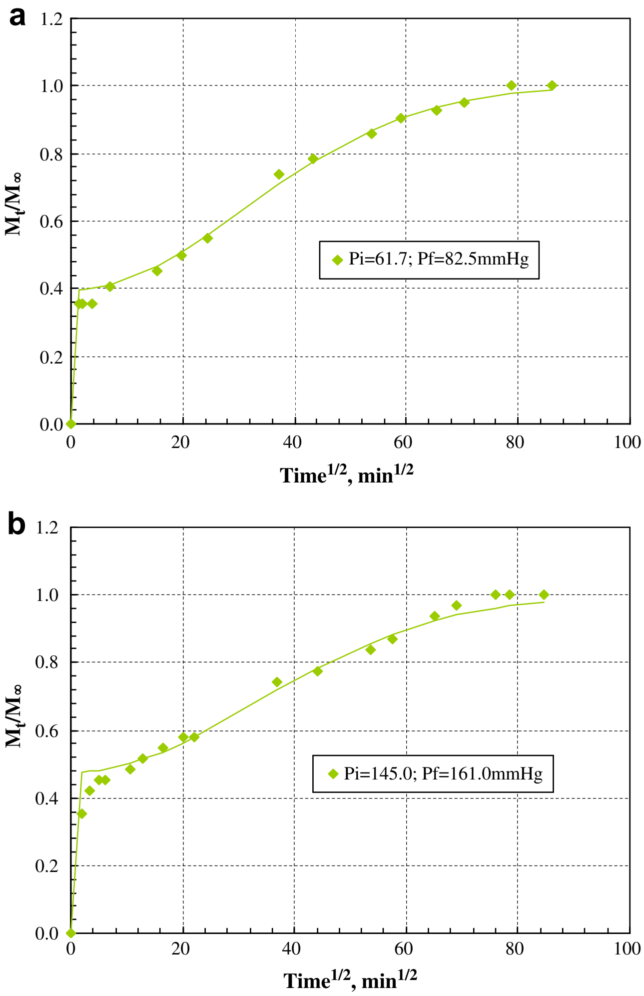

Fig. 8. Non-Fickian sorption kinetics of methanol in 1.5 micron biaxially oriented PET. Diffusion coefficient is not obtained due to very quick Fickian uptake.

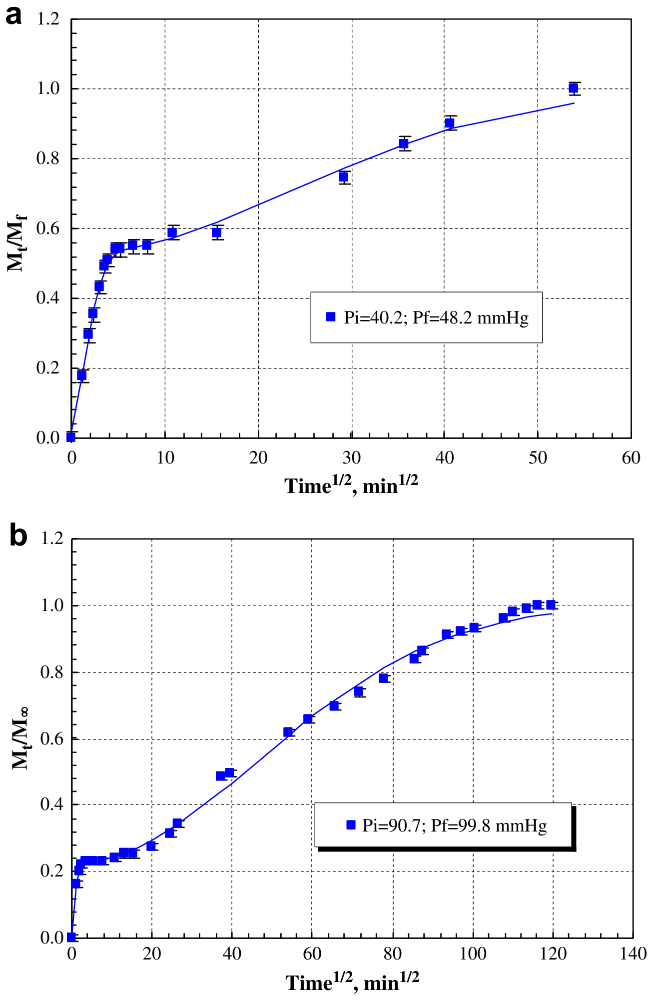

Fig. 9. Non-Fickian sorption kinetics of ethanol in 1.5 micron biaxially oriented PET.

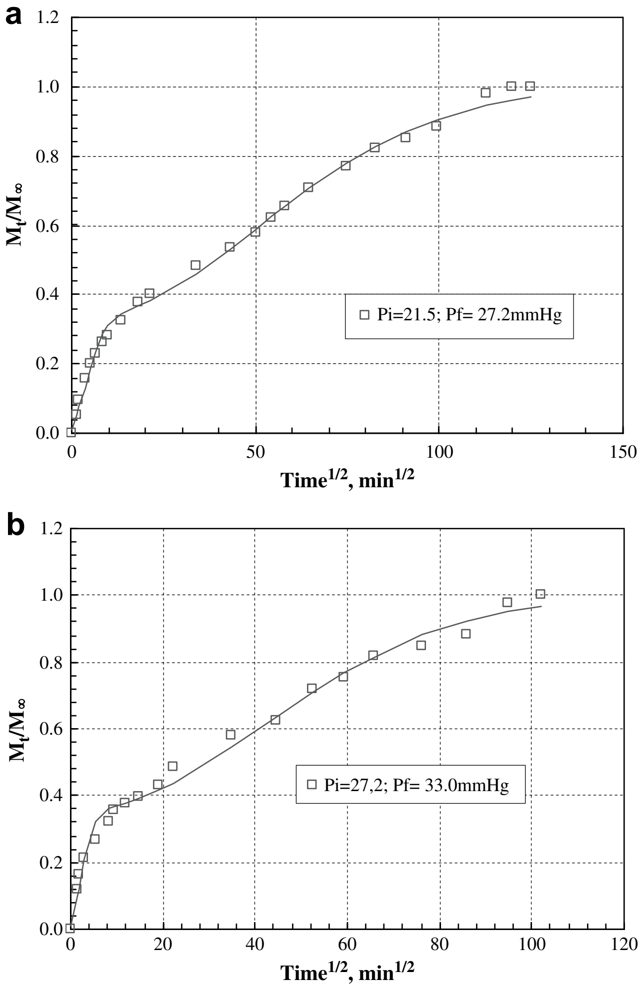

Fig. 10. Non-Fickian sorption kinetics of *n*-propanol in 1.5 micron biaxially oriented PET.

model described by equations (7)–(10) to obtain the relaxation rate constant, diffusion coefficient and fractional Fickian uptake [32]. These values are shown in Table 4. The total uptake (M_t) at any time t, can be written as

$$M_t = M_{t,\mathrm{R}} + M_{t,\mathrm{F}} \tag{7}$$

$M_{t,\mathrm{R}}$ and $M_{t,\mathrm{F}}$ are the amounts absorbed due to relaxation (subscript R) and Fickian diffusion (subscript F) respectively. $M_{\infty,F}$ is the equilibrium uptake due to Fickian diffusion. The relaxation uptake is assumed to be first order in driving force, the concentration difference between relaxation uptake at time t ($M_{t,\mathrm{R}}$) and the equilibrium uptake due to relaxation ($M_{\infty,R}$). The relaxation rate constant is k_R.

$$M_t = \phi_\mathrm{F}\left\{1-\frac{8}{\pi^2}\sum_{n=0}^{\infty}\frac{1}{(2n+1)^2}\exp\left[-(2n+1)^2 k_\mathrm{F} t\right]\right\} + (1-\phi_\mathrm{F})\,(1-\exp(-k_\mathrm{R} t)) \tag{8}$$

$$k_\mathrm{F} = \frac{\pi^2 D}{4l^2} \tag{9}$$

$$\phi_\mathrm{F} = M_{\infty,\mathrm{F}}/M_\infty \tag{10}$$

Diffusion coefficients thus obtained as a function of concentration are plotted in Fig. 12. There is a general trend of increase in the diffusivity with concentration. The strongest effect is in the case of iso-propanol, where the diffusion coefficients actually increase by two orders of magnitude over the entire activity range. Methanol diffusion coefficients cannot be obtained for the thin film because nearly 90% of the Fickian uptake happens within the first minute during which many data points cannot be taken. For comparison, therefore, diffusion coefficients from a thicker non-annealed, semicrystalline film have been shown in the plot [12]. A common form of the concentration dependence of the diffusivity is an exponential relationship as is shown in equation (11).

$$D = D_\mathrm{o}\exp(\beta C) \tag{11}$$

C is the average concentration of the penetrant in the polymer that has been calculated using the initial and final penetrant concentration. D_o represents the infinite dilution diffusion coefficient, and β is a constant. Values of the constants for the four penetrants are shown in Table 6. The concentration dependence of D is strongest for iso-propanol, the largest penetrant, and weakest for methanol, the smallest penetrant as is indicated by the increasing values of β. This would suggest much stronger concentration dependences for larger molecules. Reported values of the parameter β for linear and branched alkanes, esters and ketones suggest that the concentration dependence of the diffusion coefficient is highest for the alkanes (iso-butane, n-pentane and iso-pentane), with β being greater than 1 [1]. On the other hand, as in

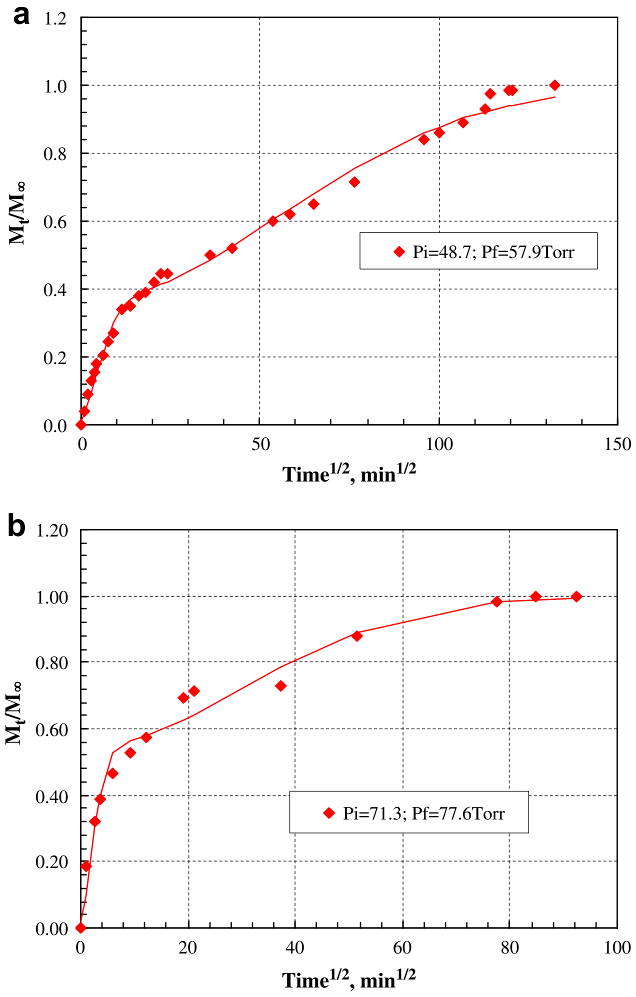

Fig. 11. Non-Fickian kinetics of *i*-propanol in 1.5 micron biaxially oriented PET.

the case of alcohols, the esters and ketones have relatively weaker concentration dependence with β being in the range of 0.3 and 0.5. This is somewhat surprising, as a more interacting penetrant would be expected to have higher concentration dependence, which, in the case of PET, would be molecules with polar groups and not the hydrocarbons. Solubility trends reinforce this expectation as the solubility of the penetrants with polar groups is higher than that of the hydrocarbons. At present, however, values reported in the literature seem to support the reverse trend of concentration dependence. It must be kept in mind that the diffusion coefficients reported here are based on the initial uptake of the penetrant, which is Fickian. Relaxation of the polymer chains thereafter implies that the diffusion coefficient of the penetrant, apart from being concentration dependent, will also be time dependent. The penetrant diffusion coefficient obtained using the Berens–Hopfenberg model is not the steady state diffusivity. Apart from being a measure of the initial diffusivity, this value is also indicative of the penetrant mobility of the polymer matrix [32]. In that sense, deviation from dual mode behavior of the sorption isotherm and swelling are consistent with the increasing diffusivity that has been measured.

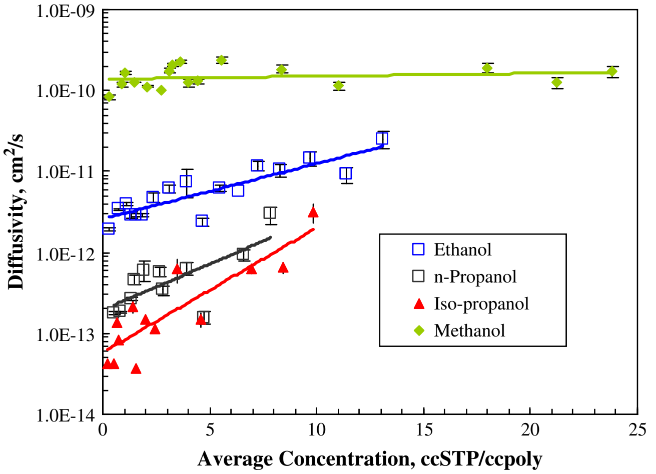

Fig. 12. Diffusion coefficient of lower alcohols as a function of the average concentration.

Table 6
Parameters defining the exponential dependence of diffusion coefficient on concentration.

Constant	D_o, cm^2/s	β, (ccSTP/ccpoly)$^{-1}$
Methanol	1.39×10^{-10}	0.008
Ethanol	2.59×10^{-12}	0.158
n-Propanol	1.95×10^{-13}	0.261
i-Propanol	5.79×10^{-14}	0.355

Based on the parameters obtained from the Berens–Hopfenberg model, certain other observations may be made. The relaxation constant, k_R is a measure of the polymer chain motion during the sorption process. Most of the relaxation constant (k_R) values are lower for *n*-propanol and *i*-propanol. All values for the penetrants studied here are of the order of 10^{-5} and 10^{-6} s^{-1}. Patton et al. report k_R of the order of 10^{-5} s^{-1} for benzene diffusion in PET [2]. Similarly, for ketones, the relaxation time constant is of the order of 10^{-5} [3]. Based on this evidence, it is difficult to draw any correlation between the relaxation rate constant and penetrant size. The fractional Fickian uptake decreases with increasing activity and concentration, and it often increases again at the high activities such as $p/p_o = 0.80$ or 0.90 due to swelling which enhances the polymer chain mobility.

4. Summary

Solubility and diffusivity of methanol, ethanol, *n*-propanol and *i*-propanol have been measured in a thin biaxially oriented PET film. Results indicated that solubility increases with increasing penetrant size and diffusivity decreases with the same. Change in the position of the hydroxyl group in propanol appears to significantly affect the diffusivity of the molecule. As a result, the diffusivity of iso-propanol is an order of magnitude lower than *n*-propanol. Such behavior may be attributed to increased width and height of the iso-propanol molecule.

It is proposed that the infinite dilution solubility of various species with the same chemical functionality correlates well with the dispersive solubility parameter. Functional groups with hydrogen bonding parameter (δ_h) closer to that of PET demonstrate a higher solubility in the polymer. The proposed correlation may be helpful in predicting the sorption properties of large flavor molecules using their solubility parameters estimated from group contribution methods [13].

Acknowledgements

The authors would like to acknowledge financial support from the Coca Cola Co. for this research.

References

[1] Dhoot SN, Freeman BD, Stewart ME. Sorption and transport of linear esters and branched alkanes in biaxially oriented poly(ethylene terephthalate). Industrial & Engineering Chemistry Research 2004;43(12):2966–76.

[2] Patton CJ, Felder RM, Koros WJ. Sorption and transport of benzene in poly(ethylene terephthalate). Journal of Applied Polymer Science 1984;29(4):1095–110.

[3] Dhoot SN, Freeman BD, Stewart ME. Sorption and transport of linear and branched ketones in biaxially oriented polyethylene terephthalate. Polymer 2004;45(16):5619–28.

[4] Dhoot SN, Freeman BD, Stewart ME, Hill AJ. Sorption and transport of linear alkane hydrocarbons in biaxially oriented poly(ethylene terephthalate). Journal of Polymer Science, Part B: Polymer Physics 2001;39(11):1160–72.

[5] Durning CJ, Rebenfeld L, Russel WB. Integral sorption with induced crystallization. Polymer Engineering and Science 1986;26(15):1066–78.

[6] Billovits GF, Durning CJ. Penetrant transport in semicrystalline poly(ethylene terephthalate). Polymer 1988;29(8):1468–84.

[7] Escoubes M, Moser D, Berticat P. Study of the sorption of 1,4-dioxane by an amorphous poly(ethylene terephthalate)glycol film and physical modifications of polymers formed by this sorption. II. Energetic aspects of the 1,4-dioxane sorption on the amorphous polymer and its exchange by ethanol. Angewandte Makromolekulare Chemie 1978;67(1):45–60.

[8] Michaels AS. Solution of gases in polyethylene terephthalate. Journal of Applied Polymer Science 1963;34(1):1–12.

[9] Koros WJ. Sorption and transport of gases in glassy polymers, Chemical engineering. Austin: University of Texas; 1977. p. 274.

[10] Chandra P. Multi-component transport of gases and vapors in poly(ethylene terephthalate). Atlanta: Department of Chemical and Biomolecular Engineering, Georgia Institute of Technology; 2006.

[11] McBain JW, Bakr AM. A new sorption balance. Journal of the American Chemical Society 1926;48:690–5.

[12] Chandra P, Koros WJ. Sorption and transport of methanol in poly(ethylene terephthalate). Polymer 2009;50(1):236–44.

[13] Immergut EH, Brandrup J. In: Handbook of polymers. 7th ed. New York: Wiley and Sons; 1989. pp. 684.

[14] Lokhandwala KA, Nadakatti SM, Stern SA. Solubility and transport of water vapor in some 6FDA-based polyimides. Journal of Polymer Science, Part B: Polymer Physics 1995;33(6):965–75.

[15] Stannett VT, Ranade GR, Koros WJ. Characterization of water vapor transport in glassy polyacrylonitrile by combined permeation and sorption techniques. Journal of Membrane Science 1982;10(2–3):219–33.

[16] Plastics Design LIbrary. In: Massey LK, editor. Permeability properties of plastics and elastomers, a guide to packaging and barrier materials. 2nd ed. Norwich: William Andrew Publishing; 2002. pp. 601.

[17] Connelly RW, McCoy NR, Koros WJ, Hopfenberg HB, Stewart ME. The effect of sorbed penetrants on the aging of previously dilated glassy polymer powders. I. Lower alcohol and water sorption in poly(methyl methacrylate). Journal of Applied Polymer Science 1987;34(2):703–19.

[18] Ranade GR, Stannett VT, Koros WJ. Kinetics of sorption and desorption for water vapor-glassy polyacrylonitrile (PAN) system. Polymer Preprints (American Chemical Society, Division of Polymer Chemistry) 1981;22(2):411–2.

[19] Yang DK, Koros WJ, Hopfenberg HB, Stannett VT. Sorption and transport studies of water in kapton polyimide. I. Journal of Applied Polymer Science 1985;30(3):1035–47.

[20] Orchard GAJ, Spiby P, Ward IM. Oxygen and water vapor diffusion through biaxially oriented poly(ethylene terephthalate). Journal of Polymer Science, Part B: Polymer Physics 1990;28(5):603–21.

[21] Wibawa G, Watano R, Sato Y, Takoshima S, Masuoka S. Solubilities of 11 polar organic solvents in four polymers using the piezoelectric-quartz sorption method. Journal of Chemical and Engineering Data 2002;47(4):1022–9.

[22] Hopfenberg HB, Nicolais L, Drioli E. Relaxation controlled (case II) transport of lower alcohols in poly(methyl methacrylate). Polymer 1976;17(3):195–8.

[23] Bauer K, Garbe D, Surburg H. Common fragrance and flavor materials. 3rd ed. Weinheim: Wiley-VCH; 1997. pp. 278.

[24] McDowell CC, Freeman BD, McNeely GW. Acetone sorption and uptake kinetics in poly(ethylene terephthalate). Polymer 1999;40(12):3487–99.

[25] Koros WJ, Chan AH, Paul DR. Sorption and transport of various gases in polycarbonate. Journal of Membrane Science 1977;2(2):165–90.

[26] Reid RC, Prausnitz JM, Poling BE. The properties of gases and liquids. 4th ed. New York: mcGraw Hill; 1987.

[27] Berens AR, Hopfenberg HB. Diffusion of organic vapors at low concentrations in glassy PVC, polystyrene, and PMMA. Journal of Membrane Science 1982;10(2-3):283–303.

[28] Serad GE, Freeman BD, Stewart ME, Hill AJ. Gas and vapor sorption and diffusion in poly(ethylene terephthalate). Polymer 2001;42(16):6929–43.

[29] Hopfenberg HB, Holley RH, Stannett V. The effect of penetrant activity and temperature on the anomalous diffusion of hydrocarbons and solvent crazing in polystyrene. Polymer Engineering and Science 1969;9(4):242.

[30] Berens AR. Diffusion and relaxation in glassy polymer powders. 1. Fickian diffusion of vinyl chloride in poly(vinyl chloride). Polymer 1977;18(7):697–704.

[31] Moaddeb M, Koros WJ. Effects of orientation on the transport of D-limonene in polypropylene. Journal of Applied Polymer Science 1995;57(6):687–703.

[32] Berens AR, Hopfenberg HB. Diffusion and relaxation in glassy polymer powders. 2. Separation of diffusion and relaxation parameters. Polymer 1978;19(5):489–96.

[33] Perry RH, Green DW. Perry's chemical engineer's handbook. 6th ed. New York: McGraw-Hill; 1984. pp 3-55.

[34] Barton AF. CRC handbook of polymer–liquid interaction parameters and solubility parameters. Boca Raton, FL: CRC Press; 1990.

[35] Aref-Azar A, Arnoux F, Biddlestone F, Hay JN. Physical aging in amorphous and crystalline polymers. Part 2. Poly(ethylene terephthalate). Thermochimica Acta 1996;273:217–29.

[36] Yasuda H, Stannett V. Permeation, solution, and diffusion of water in some high polymers. Journal of Polymer Science 1962;57:907–23.

[37] Bove L, D'Aniello C, Gorrasi G, Guadagno L, Vittoria V. Transport properties of the mesomorphic form of poly(ethylene terephthalate). Polymer 1996;37(23):5309–11.